Mutations in Orai1 transmembrane segment 1 cause STIM1-independent activation of Orai1 channels at glycine 98 and channel closure at arginine 91

Shenyuan L. Zhang[a,b,1,2], Andriy V. Yeromin[a,1], Junjie Hu[c], Anna Amcheslavsky[a], Hongying Zheng[b], and Michael D. Cahalan[a,d,2]

[a]Department of Physiology and Biophysics and [d]Center for Immunology, University of California, Irvine, CA 92697; [b]Department of Systems Biology and Translational Medicine, Texas A&M Health Science Center, Temple, TX 76504; and [c]Department of Genetics and Cell Biology, College of Life Sciences and Tianjin Key Laboratory of Protein Sciences, Nankai University, Tianjin 300071, China

Contributed by Michael D. Cahalan, September 8, 2011 (sent for review August 5, 2011)

Stim and Orai proteins comprise the molecular machinery of Ca^{2+} release-activated Ca^{2+} (CRAC) channels. As an approach toward understanding the gating of Orai1 channels, we investigated effects of selected mutations at two conserved sites in the first transmembrane segment (TM1): arginine 91 located near the cytosolic end of TM1 and glycine 98 near the middle of TM1. Orai1 R91C, when coexpressed with STIM1, was activated normally by Ca^{2+}-store depletion. Treatment with diamide, a thiol-oxidizing agent, induced formation of disulfide bonds between R91C residues in adjacent Orai1 subunits and rapidly blocked STIM1-operated Ca^{2+} current. Diamide-induced blocking was reversed by disulfide bond-reducing agents. These results indicate that R91 forms a very narrow part of the conducting pore at the cytosolic side. Alanine replacement at G98 prevented STIM1-induced channel activity. Interestingly, mutation to aspartate (G98D) or proline (G98P) caused constitutive channel activation in a STIM1-independent manner. Both Orai1 G98 mutants formed a nonselective Ca^{2+}-permeable conductance that was relatively resistant to block by Gd^{3+}. The double mutant R91W/G98D was also constitutively active, overcoming the normal inhibition of channel activity by tryptophan at the 91 position found in some patients with severe combined immunodeficiency (SCID), and the double mutant R91C/G98D was resistant to diamide block. These data suggest that the channel pore is widened and ion selectivity is altered by mutations at the G98 site that may perturb α-helical structure. We propose distinct functional roles for G98 as a gating hinge and R91 as part of the physical gate at the narrow inner mouth of the channel.

store-operated Ca^{2+} entry | gating mechanism | Ca^{2+}

Store-operated Ca^{2+} entry (SOCE) leads to refilling of Ca^{2+} content within the endoplasmic reticulum (ER) following inositol trisphosphate-mediated Ca^{2+} release (1). In T lymphocytes and other hematopoietic cells, depletion of Ca^{2+} from within the ER Ca^{2+} store activates Ca^{2+} release-activated Ca^{2+} (CRAC) channels and amplifies cytosolic Ca^{2+} signaling following receptor engagement, leading to changes in gene expression that regulate immune responses (2, 3). STIM and Orai proteins were discovered in RNA interference screens as the two essential components that underlie CRAC channel function (4–8). The human genome contains two STIM (STIM1 and STIM2) and three Orai (Orai1, Orai2, and Orai3) genes. Orai1, with four transmembrane (TM) segments in the plasma membrane (PM), is the CRAC channel pore-forming subunit in T lymphocytes (4, 7–11), and STIM1 with one TM segment serves as the ER Ca^{2+} sensor/activation subunit that opens CRAC channels in the PM (5, 6, 12, 13).

The functional CRAC channel is unusual in having an extremely low single-channel conductance and is highly selective for Ca^{2+} ions (14–16). Available evidence indicates that the channel conducts as a tetramer of Orai1 subunits (17–21). Site-directed mutagenesis confirmed *Drosophila* Orai and human Orai1 as pore-forming subunits by identifying conserved glutamate residues near the extracellular side of TM1 of Orai (E180) or Orai1 (E106) that confer Ca^{2+} selectivity on the STIM-operated Orai current (9–11, 22). Mutations of STIM1 and Orai1 have been shown to cause severe combined immunodeficiency (SCID) in human patients (4, 23, 24). In particular, Orai1 R91, the site of the originally described SCID mutation (4)—R91W near the cytosolic side of the first TM segment (TM1)—has been investigated by site-specific mutagenesis (4, 19, 25).

Several studies have elucidated the chain of events that link Ca^{2+} release from the ER to activation of CRAC channels in the PM. Upon ER Ca^{2+}-store depletion, STIM1 unbinds Ca^{2+} and translocates to ER junctions adjacent to the PM, where a C-terminal domain of STIM1 interacts with Orai1 cytosolic domains, opening the Orai1 channel and causing Ca^{2+} influx (26). Recent studies using cysteine scanning combined with blocker accessibility and disulfide cross-linking studies suggest an α-helical structure in Orai1 TM1 (27, 28). Nevertheless, the molecular events following STIM1–Orai1 interaction that lead to channel opening remain elusive, and the gating determinants within Orai1 are undefined.

In this study, we sought to explore elements within Orai1 that control channel gating by biochemical and functional analysis of Orai1 point mutants. We analyzed mutations of arginine 91 to determine whether oxidation of R91C could form disulfide bonds between adjacent Orai1 subunits and block channel function. Furthermore, we explored mutations of Orai1 at the conserved glycine residue in the middle of TM1 (G98) and found either dominant-negative inhibition or robust spontaneous activation of Orai1 proteins as functional channels (store- and STIM1-independent), depending on the amino acid substitution. Biophysical analysis indicated a distinct channel open state with altered ion selectivity in spontaneously active G98 mutants. We further analyzed double mutants bearing both inhibitory and activating mutations at R91 and G98 sites, respectively, to determine whether R91W or G98D effects are dominant. Our data suggest that R91 forms a very narrow part of the conducting pore at the cytosolic side of TM1, and that G98, in the middle of TM1, is likely to serve as a gating hinge of Orai1 channels.

Results

Bulky Hydrophobic Side Chains at R91 Inhibit Orai1 Channel Activity. We initially screened several Orai1 R91 point mutants by Ca^{2+}

Author contributions: S.L.Z., A.V.Y., J.H., and M.D.C. designed research; S.L.Z., A.V.Y., A.A., and H.Z. performed research; S.L.Z. and A.V.Y. analyzed data; and S.L.Z., A.V.Y., and M.D.C. wrote the paper.

The authors declare no conflict of interest.

[1]S.L.Z. and A.V.Y. contributed equally to this work.

[2]To whom correspondence may be addressed. E-mail: shenyuan.zhang@medicine.tamhsc.edu or mcahalan@uci.edu.

This article contains supporting information online at www.pnas.org/lookup/suppl/doi:10.1073/pnas.1114821108/-/DCSupplemental.

imaging in transfected HEK-293A cells. Expression levels and PM localization of wild-type (WT) Myc-tagged Orai1 and Orai1 R91 mutants were similar, based upon immunofluorescence (Fig. S1) and Western blotting. In cells cotransfected with STIM1 and WT Orai1, thapsigargin (TG) treatment produced elevation of cytosolic Ca^{2+} concentrations ($[Ca^{2+}]_i$) to more than 800 nM (863 ± 42 nM, n = 77 cells; Fig. 1*A*), much greater than the endogenous SOCE in control cells transfected with green fluorescent protein (GFP) only (264 ± 15 nM, n = 81 cells; Fig. S2*A*). In agreement with previous studies (4, 19, 25), substitution with tryptophan at R91, namely the SCID mutation Orai1 R91W, inhibited Ca^{2+} entry to below the endogenous level (124 ± 31 nM, n = 25 cells). Among other amino acid substitutions tested (Fig. 1*A* and Fig. S2), smaller amino acids such as alanine, glycine, or cysteine all promoted Ca^{2+} influx to levels similar to wild-type (883 ± 89 nM, 21 cells for R91A; 628 ± 40 nM, 20 cells for R91G; 575 ± 56 nM, 26 cells for R91C). Moreover, charge-conserving and even charge-reversing amino acid substitutions also promoted Ca^{2+} entry (904 ± 127 nM, 15 cells for R91K; 1,037 ± 131 nM, 24 cells for R91D). However, similar to R91W, substitution with leucine (R91L) did not support SOCE (250 ± 36 nM, 12 cells). These results are consistent with previous studies (4, 25) showing that only bulky hydrophobic amino acid substitutions at R91 inhibit Orai1 channel function.

R91C on Adjacent Subunits Can Form Disulfide Bonds, Blocking Orai1 Channel Activity. To test the idea that R91 residues on adjacent subunits are sufficiently close together that a bulky hydrophobic amino acid substitution could physically occlude the channel or prevent opening, we tested for the ability of functional R91C channels to form disulfide bonds. Intact HEK-293A cells expressing functional WT or R91C Orai1 were treated with diamide, an oxidant that catalyzes disulfide-bond formation between nearby cysteine residues (Fig. 1*B*). Wild-type Orai1 proteins were detected primarily as a monomer band, consistent with its predicted molecular weight (~34 kDa) with or without diamide treatment. We note that even without diamide treatment, there was some residual level of Myc-Orai1 oligomers from both wild-type and R91C mutants, most likely due to the higher-order stoichiometry of Orai1 as membrane proteins with dimer or tetramer structure in intact cells (18, 20, 29, 30), along with incomplete dissociation during cell-lysate treatment. However, for R91C, diamide treatment caused the monomer band to disappear as a strong band at higher molecular weight emerged, consistent with covalent dimer formation. The dimers reverted to monomers following incubation of cell lysates with dithiothreitol (DTT), confirming disulfide-bond formation. These results suggested that cysteine residues at position 91 on adjacent subunits may come close enough to form disulfide bridges.

To rule out the possibility that the R91C dimers were formed by disulfide bonds between 91C and cysteine residues elsewhere within Orai1, the three intrinsic cysteine residues were mutated to serine to generate a cysteine-less Orai1 mutant (C-less Orai1). C-less Orai1 functioned in Ca^{2+}-imaging experiments exactly as wild-type (Fig. 1*A*) and did not form diamide-induced dimers. Indeed, we confirmed as expected that the R91C mutant of C-less Orai1 also formed dimers when incubated with diamide (Fig. 1*C*). Moreover, upon diamide treatment, the GFP-tagged WT Orai1 was present as a monomer of the expected molecular weight (~61 kDa), whereas R91C GFP-Orai1 showed a strong dimer band with a higher molecular weight (~122 kDa; Fig. 1*D*). These results exclude the possibility that the indicated Orai1 dimer band in Fig. 1*B* was not formed by R91C Orai1 homodimers but by disulfide bonds between exogenous Orai1 and some endogenous proteins similar in size to Orai1. Together, these data reinforce the conclusion that Cys residues at position 91 on adjacent Orai1 subunits are sufficiently close to form disulfide linkages.

Functional effects of diamide treatment on Orai1 channel activity were further examined by Ca^{2+} imaging and whole-cell current recording. Application of 1–10 mM diamide inhibited TG-evoked Ca^{2+} influx through R91C Orai1, but had little effect on WT Orai1 (Fig. 2 *A* and *B* and Fig. S3). Diamide-induced blockage of R91C Orai1 was quickly reversed by application of the reducing agent DTT. These results demonstrate that disulfide-bond formation between adjacent R91C sites blocks Orai1 channel activity. Moreover, treatment with diamide during TG application also nearly abolished Ca^{2+} influx through R91C channels but not WT Orai1 channels, indicating that Ca^{2+} influx through the channel is not required for the diamide block (Fig. 2 *C* and *D* and Fig. S3). Again, treatment with DTT reversed the diamide block and restored Ca^{2+} influx through R91C channels, but had only a mild effect on WT channels. Fig. 2 *E* and *F* shows the effect of diamide on STIM1-induced R91C Orai1 whole-cell current activated by passive store depletion during pipette dialysis with 12 mM 1,2-bis(*o*-aminophenoxy)ethane-N,N,N',N'-tetraacetic acid (BAPTA). As expected, following the typical activation of CRAC-like current, elevation of external Ca^{2+} increased the inwardly rectifying current amplitudes. Following some current rundown (before trace 1), diamide treatment (10 mM) rapidly blocked the current (trace 2). Subsequent treatment with a reducing agent, bis(2-mercaptoethyl)sulfone (BMS) (5 mM), partially restored the R91C current (traces 3 and 4), consistent with a reduction of disulfide bonds formed during diamide treatment. In cells cotransfected with WT Orai1 plus STIM1, diamide partially suppressed the current by 32 ± 14% (n = 4); but unlike its effect on the R91C Orai1 current, diamide block was completely reversible upon washout. Collectively, our Ca^{2+}-imaging and patch-clamp data indicate that di-

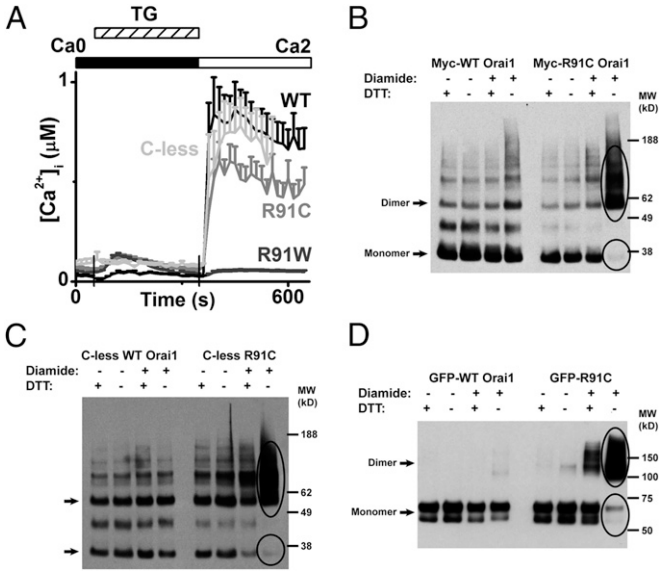

Fig. 1. Diamide treatment induces R91C to form homo-disulfide bonds. (*A*) $[Ca^{2+}]_i$ responses (mean ± SE) before and following store depletion by addition of 2 μM TG to HEK cells transfected with STIM1 + Myc-Orai1 (positive control; n = 5 cells), STIM1 + R91W Myc-Orai1 (n = 8 cells), STIM1 + C-less Myc-Orai1 (n = 4 cells), and STIM1 + R91C Myc-Orai1 (n = 10 cells). Data shown are representative of at least three experiments with >15 cells for each condition. Vertical lines indicate the time of solution exchange. Ca0 indicates zero free Ca^{2+}; Ca2 indicates 2 mM Ca^{2+} (Table S1). (*B*) Representative Western blotting (n = 4) of Myc-tagged WT Orai1 and R91C Orai1 from cells treated without or with 10 mM diamide; total cell lysates were boiled either with or without DTT (100 mM, 10 min at 70 °C). MW refers to molecular weight markers (kDa). (*C*) Representative Western blotting of Myc-tagged C-less Orai1 and C-less R91C Orai1 from cells treated with or without diamide and DTT. (*D*) Representative anti-GFP Western blotting of cell lysates with overexpressed GFP-Orai1 and R91C GFP-Orai1 proteins.

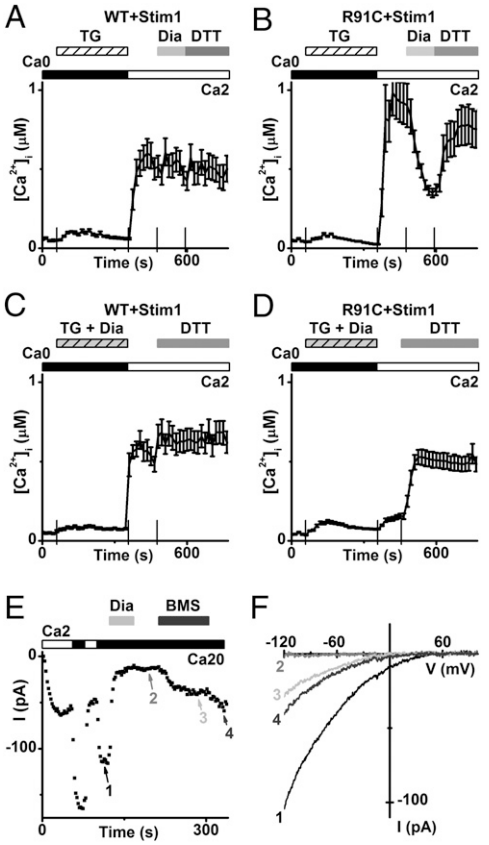

Fig. 2. R91C Orai1 channels are blocked by oxidation treatment. (*A* and *B*) $[Ca^{2+}]_i$ responses (±SE) before and following store depletion by addition of 2 μM TG. Effect of diamide (Dia) (1 mM) and following DTT (2 mM) application on Ca^{2+} influx in cells cotransfected with STIM1 and either WT Orai1 or R91C Orai1 (n = 5 and 8 cells, respectively). (*C* and *D*) Pretreatment with diamide (1 mM) has no effect on WT Orai1 but prevents Ca^{2+} influx through R91C Orai1 (n = 7 cells for each). DTT restores Ca^{2+} influx through R91C channels. (*E*) Representative result for block of R91C Orai1 CRAC current by diamide treatment (10 mM, n = 13 cells); recovery upon BMS treatment (5 mM, n = 6 cells). Traces are leak-subtracted; the current at break-in was considered as the leak. (*F*) Corresponding I-V curves for the time points indicated in *E*.

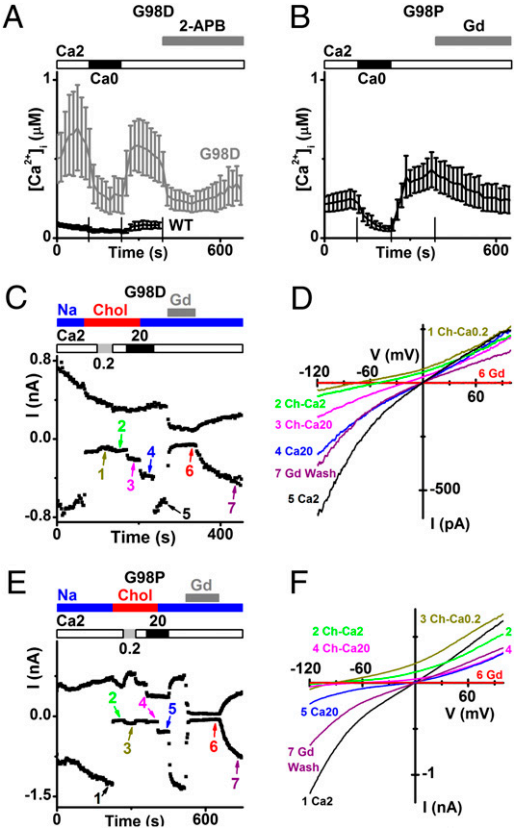

Fig. 3. G98 mutants form spontaneously activated Orai1 channels. (*A*) Resting $[Ca^{2+}]_i$ in cells expressing WT Orai1 without STIM1 (n = 8 cells) or in cells expressing G98D Orai1 (n = 7 cells). Representative data are shown; average values include 46 ± 4 nM, 41 cells for WT Orai1; 260 ± 28 nM, 81 cells for G98D; $P < 0.0001$ for WT compared with G98D; $P < 0.0001$ for Ca2 compared with Ca0 in 44 cells transfected with G98D. 2-APB application (50 μM). (*B*) Resting $[Ca^{2+}]_i$ in cells expressing G98P Orai1 (n = 8 cells); 190 ± 42 nM, 14 cells for G98P; $P <$ 0.0001 for WT compared with G98P; P = 0.0032 for Ca2 compared with Ca0 in 14 G98P cells. Gd^{3+} application (10 μM). (*C*) Time course of inward and outward G98D Orai1 currents, measured at −120 and +100 mV, respectively. Currents are representative of six experiments. Chol, choline. (*D*) Corresponding I-V relationships. Numbered traces and colors correspond to times indicated in *C*. (*E* and *F*) Time course and I-V relationships of G98P Orai1 currents. Currents are representative of four experiments.

amide treatment induces disulfide-bond formation in adjacent Orai1 R91C subunits and blocks functional channel activity.

G98D and G98P Orai1 Form Spontaneously Active Ca^{2+} Channels in the Absence of STIM1. In the middle of the predicted TM1 α-helix, a conserved glycine residue (G98) is predicted to be located exactly two α-helical turns from the R91 site. We hypothesize that glycine could provide conformational flexibility in TM1 to open Orai1 channels upon interaction with STIM1. A series of mutants with alanine substitutions was generated around this 98 site; all were well-expressed as examined by immunofluorescence (Fig. S1) and Western blotting, and were evaluated by Ca^{2+} imaging. Expression of G98A Orai1 with STIM1 failed to exhibit channel activity, suggesting an important role of the original Gly at this position. Indeed, G98A Orai1 completely inhibited endogenous SOCE (Fig. S4*C*; peak: 74 ± 16 nM, 18 cells; $P < 0.0001$ compared with peak of control cells, as shown in Fig. S2*A*); this may indicate a dominant-negative action by subunit assembly with endogenous WT Orai1 subunits. To further investigate the role of glycine at position 98, we generated mutations that might perturb structure in TM1 by substitution with negatively charged aspartate. We also tested whether the presence of a proline at position 98 may induce spontaneous channel activity. Strikingly, G98D and G98P mutants each resulted in constitutive Orai1 channel activation (Fig. 3 *A* and *B*). Even when expressed alone, and without the requirement for TG-evoked store depletion, G98D and G98P Orai1 mutants caused a dramatic elevation of resting $[Ca^{2+}]_i$ compared with WT. The elevated resting Ca^{2+} induced by both mutants was reduced by application of 2-aminoethyl diphenylborinate (2-APB) or Gd^{3+}. Possibly as a result of the abnormally high cytosolic free Ca^{2+}, most G98D- and G98P-expressing cells were killed within 2 d after transfection.

Altered Open Channel Properties in Constitutively Active G98D and G98P Orai1 Mutants. To permit detailed functional evaluation of ion selectivity, we protected G98D-expressing cells from death by treatment with 10 μM La^{3+} (*SI Materials and Methods*) and analyzed G98D Orai1 spontaneous channel activity (Fig. 3*C*). Unlike the WT Orai1 mutant, neither G98D nor G98P required STIM1 coexpression to produce robust currents. In contrast to CRAC-like inwardly rectifying current-voltage (I-V) curve with its characteristic positive reversal potential, the current induced by G98D was nearly linear, with a reversal potential close to 0 mV and an outward component carried by Cs^+ (Fig. 3*D*, black trace). Ion-substitution experiments, using choline to replace Na^+ and varying

external Ca^{2+} concentration, revealed a substantial inward Na^+ current component (Fig. 3*D*, green trace), along with a small component of inward Ca^{2+} current (Fig. 3*D*, magenta trace; data summary in Fig. S5). The current sensitivity to block by Gd^{3+} was considerably reduced compared with WT; the half-blocking concentration was 310 nM for G98D and 7 nM for WT Orai1 (Fig. S6). Finally, by noise analysis, the large G98D monovalent currents reflect a greatly increased single-channel conductance of ~9 pS for G98D Orai1 compared with <10 fS for STIM1-operated Ca^{2+}-selective WT Orai1 (Fig. S7).

To test whether a charged residue at G98 is required for spontaneous nonselective currents, we evaluated proline substitution to disrupt the α-helical TM1 structure. G98P Orai1 constitutively active channels showed closely similar but not identical biophysical properties to G98D (Fig. 3*E*). Resembling G98D, the G98P Orai1 I-V relationship in normal Ringer solution exhibited only slight inward rectification with a reversal potential close to 0 mV (Fig. 3*F*, black trace). Substitution of choline for Na^+ revealed a predominance of inward monovalent Na^+ current (Fig. 3*F*, green and magenta traces). However, unlike G98D Orai1, Ca^{2+} ions blocked the G98P channels; in the presence of choline as the major cation, reduction of Ca^{2+} from 2 to 0.2 mM increased both inward and outward currents (Fig. 3 *E* and *F*, gold trace). Changing external $[Ca^{2+}]_o$ from 2 to 20 mM slightly increased the inward current for G98P, suggesting that the G98P channel does conduct Ca^{2+} to a limited extent, but less than in G98D (data summary in Fig. S5). Similar to G98D Orai1, 10 μM Gd^{3+} potently and reversibly blocked the G98P current ($n = 3$). In summary, our analysis of ion selectivity indicates that proline or aspartate at position 98 induces spontaneous Orai1 channel activity that is nonselective for monovalent cations. Ca^{2+} is sparingly permeant in G98D, but acts primarily to block monovalent currents in G98P.

Dominance of G98D. Orai1 double mutants were then generated to address the question of whether a G98-activating mutation can change the Orai1 channel phenotypes of R91W (nonconducting channels) and R91C (diamide-induced disulfide bonds and channel block). In the double mutants R91W/G98D and R91C/G98D, the presence of G98D appeared to dominate in eliciting large, spontaneously active current with nearly linear I-V shapes and modified ion selectivity. As in the G98D single mutant, STIM1 expression was not required for channel function. In the double mutant R91W/G98D, we noted spontaneous current with similar, although not identical, biophysical characteristics (Fig. 4 *A* and *B*), compared with the single mutant G98D Orai1 (Fig. 3 *C* and *D*). Again, substitution of Na^+ by choline considerably reduced the inward current amplitudes, indicating a predominantly Na^+-selective channel. The presence of significant outward current indicates that Cs^+ is also permeant. However, for the R91W/G98D double mutant, varying external Ca^{2+} concentration did not produce changes consistent with measurable Ca^{2+} permeability. The contribution of Ca^{2+} ions was just 3 ± 1% of the total current, compared with 7 ± 1% for G98D (Fig. S5). Our results indicate that despite the presence of the bulky SCID-inducing tryptophan at position 91, the presence of G98D restores channel activity, albeit with reduced Ca^{2+} permeability. Next, we examined R91C/G98D currents (Fig. 4 *C* and *D*). Again, double-mutant channels were spontaneously active with fairly linear I-V characteristics, and results from choline substitution indicated a predominance of Na^+ inward current. Varying external Ca^{2+} concentration clearly produced changes in current consistent with a measurable contribution of Ca^{2+} current. Most importantly, R91C/G98D was not efficiently blocked by diamide (Fig. 4 *E* and *F*); note that neither diamide nor BMS had any detectable effect on R91C/G98D current. These results indicate that the presence of G98D widens and activates the pore to conduct with altered ion selectivity; moreover, they reinforce the suggestion that the G98 sites of Orai1 may serve as gating hinges for channel opening and closing.

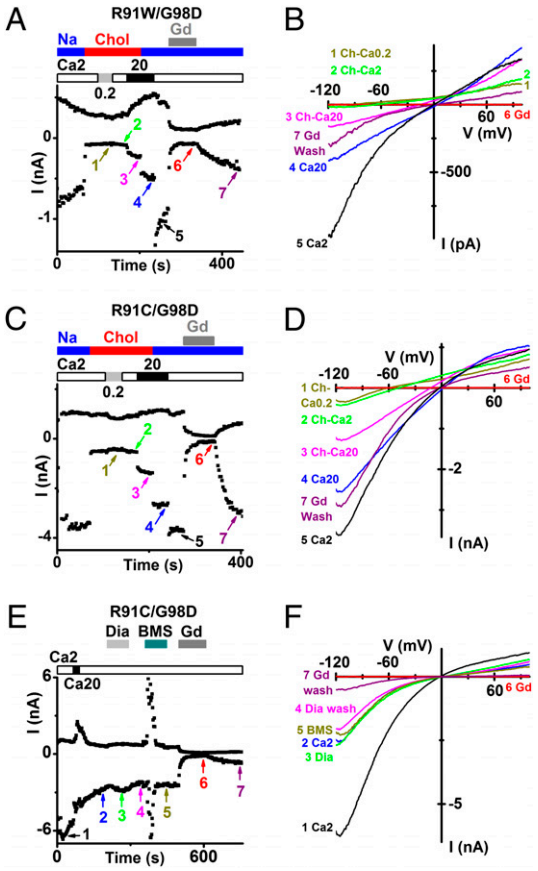

Fig. 4. Dominance of G98D mutation. (*A*) G98D restores channel activity of R91W Orai1. Expression of R91W/G98D Orai1 results in preactivated cationic current. (*B*) Corresponding I-V curves for conditions indicated in *A*. (*C* and *D*) Properties of nonselective R91C/G98D Orai1 current: cationic permeability (*C*) and corresponding I-V relationships (*D*). (*E*) Diamide application does not suppress R91C/G98D current ($n = 3$ cells). (*F*) Corresponding I-V curves for the time points indicated in *E*.

Discussion

In this study, we characterize a gain-of-function Orai1 mutation (G98D) that spontaneously opens the channel and mediates Ca^{2+} entry without store release and without coexpression of STIM1 or STIM1 fragments. Based on single-cell Ca^{2+}-imaging and patch-clamp data, we speculate that both G98D and G98P mutants are locked in an open channel conformation, due to a structural change in the middle of the Orai1 TM1 helix caused by aspartate or proline substitution. This may result in the normal channel "gate" near or at R91 being opened at the cytosolic (inner) end of TM1. We further hypothesize that the original Gly residue at the 98 site serves functionally as a "gating hinge," switching channel conformations between the closed state and the open state.

Structural and functional evidence for gating hinges at transmembrane glycine residues has been reported previously in the voltage gated-like channel superfamily that includes voltage-gated K^+, Na^+, and Ca^{2+} channels (31–33). Moreover, substitutions of aspartate or proline in transmembrane helices have been shown to cause constitutive activation of voltage-gated channels (34, 35). However, in these instances, ion selectivity does not change when gating is perturbed, consistent with a rigid selectivity filter in the voltage gated-like channels. The Orai channel family bears no sequence or structural resemblance to these channels. However, our results suggest that glycines in TM1 may play a key role in the gating of the Orai1 channel and that ion selectivity is not rigidly defined as for voltage gated-like channels.

Based on structural knowledge from potassium and sodium channels (31, 36), our results and interpretations can be formulated into a hypothetical gating mechanism (Fig. 5*A*). The Orai channels are multitransmembrane proteins that form a tetrameric pore (18, 20, 29), and it is reasonable to propose that the Orai1 channel has a very narrow part (gate) within its pore that prevents ion conductance in the closed state. In the open state, this very narrow part is pulled away by the surrounding α-helices. The G98 sites are very likely to be responsible for this conformational change upon channel activation. This is supported by the fact that the G98 residue is the only one along the Orai1 TM1 fragment that provides relatively large flexibility on the backbone dihedral angles for conformational changes. A recent report also suggested that the N-terminal half (inner side) of TM1 has rotational mobility potential or flexibility of the protein backbone (27). Moreover, we show that alanine substitution inhibits channel activation, whereas more perturbing substitutions—aspartate or proline—result in constitutive channel activation.

We also demonstrate that the R91 sites on adjacent Orai1 subunits can be cross-linked by oxidation of cysteines, allowing the relative distance between R91 sites to be estimated functionally by biochemical analysis and in real-time while Ca^{2+} imaging or during a patch-clamp experiment. The ability of R91C Orai1 to form disulfide bonds between neighboring subunits, even in a cysteine-less background, clearly demonstrates that this site forms a very narrow ring at the cytosolic side of the channel. Our data suggest that during dynamic fluctuation, the adjacent thiol side chains from 91 sites could approach each other. Moreover, they imply that bulky hydrophobic amino acid substitutions, such as the R91W mutation in humans that causes SCID, physically occlude the pore at the cytosolic side of the channel (Fig. 5*B*). In other words, a greasy plug results in a dead channel. The physical distance between the R91 side chains within a WT Orai1 channel may be greater than in R91C, given the electrostatic repulsion that would create. However, the similarity in function of R91C Orai1 channels to WT indicates that cysteine replacement at site 91 does not significantly change the overall structure and the gating mechanism of Orai1 channels. Two facts support the idea that Orai1 channels close their inner gate in the resting state: R91C can be cross-linked by diamide, and R91G or R91A Orai1 channels with even shorter side chains do not open spontaneously. These results suggest that conformational changes on the cytosolic half of TM1 (below the 98 site) open the channel, the glycine hinge at site 98 providing flexibility to open the inner gate upon STIM1 interaction. Our results and interpretations are consistent with previous reports that bulky hydrophobic residues impair the gating of Orai1 channels but do not greatly perturb the dynamic coupling between STIM1 and R91W Orai1 (25, 37).

Turning to the control of ion selectivity in the Orai1 channel, recent cysteine-scanning studies focusing on the TM1 region of Orai1 support a predicted α-helical structure with three additional sites (S88, L95, and V102) that may face the pore lumen (27, 28). A tetrameric structure for the open channel with several rings aligned from top to bottom forming a long and narrow conducting pore may well explain the extremely low conductance (~10 fS) of native or expressed CRAC current. At the top of TM1, a conserved glutamate residue (E106) is thought to determine Ca^{2+} selectivity because a relatively minor point mutation that shortens the side chain by one carbon atom (E106D Orai1, or E180D in *Drosophila* Orai) promotes nonselective cation permeability, including Cs^{+} with a diameter of 3.3 Å (9–11). Because E106D channels with a widened selectivity filter do not open spontaneously, we suggest that the opening of the G98D mutant channel is associated with increased distance between TM1 helices, including an enlarged opening at the cytosolic end of TM1. Pore dilation from top to bottom would thus result in a nonselective and constitutively active "leaky" channel associated with higher single-channel conductance and reduced sensitivity to block by Gd^{3+} (Fig. 5*C*). This is further supported by the results from the double mutants. R91W Orai1 does not normally conduct even when the channels are in the open state and engaged by STIM1 after store depletion (25, 37). The bulky hydrophobic side chains from the tryptophan residues prevent Ca^{2+} influx, permanently closing the channels. G98D double mutants are also spontaneously active, and the fact that G98D can overcome the silent-channel phenotype of R91W channels in the R91W/G98D double mutant further suggests that the cytosolic side of TM1 is dilated by the G98D mutation (Fig. 5*D*), leading to constitutively open and nonselective channels. Furthermore, we showed that the R91C/G98D double mutant forms a nonselective cation channel that is resistant to diamide-induced block, again consistent with an overall dilation of the open channel produced by G98D.

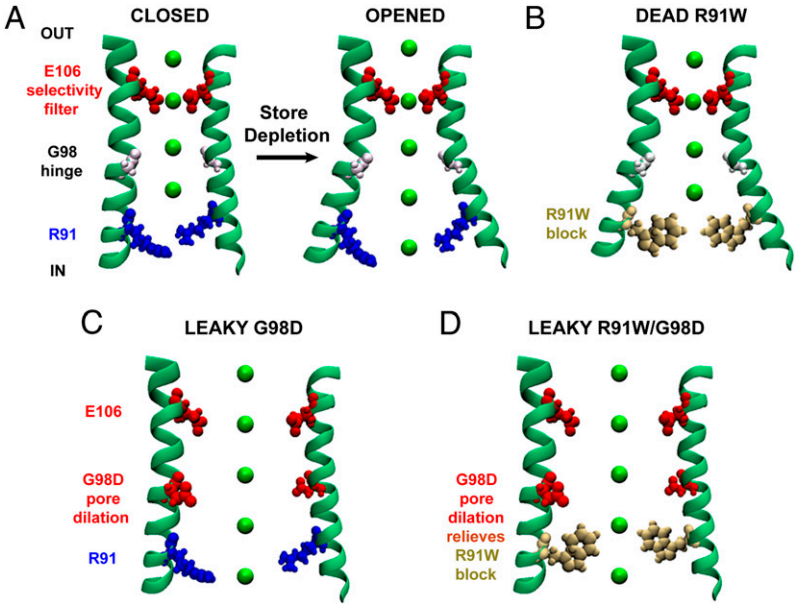

Fig. 5. Schematic models of Orai1/CRAC channel gating. Two of the pore-lining Orai1 TM1 segments are shown, with E106, G98, and R91 highlighted from outside to inside. (*A*) E106 sites near the outside control Ca^{2+} selectivity. The open pore has a diameter <3.3 Å, the diameter of an impermeant Cs^{+} ion. Near the inside, the R91 sites prevent ion flow in the closed state of the channel. Located in the middle of TM1, the G98 sites permit a conformational change that opens the channel upon store depletion followed by STIM1–Orai1 interaction. (*B*) R91W Orai1, irreversibly closed by a greasy tryptophan plug and hence a "dead" channel. (*C*) Spontaneously open G98D Orai1, with a dilated pore allowing nonselective currents (leaky) to permeate. (*D*) G98D/R91W double mutant, spontaneously open and leaky, allowing monovalent cation permeation despite tryptophan at position 91.

Studies of STIM/Orai coupling have led to an increasingly reductionist approach to understanding CRAC channel gating (26). The field has discovered progressively simpler ways to activate CRAC currents from receptor-mediated intracellular signaling pathways to ER Ca^{2+}-store depletion itself as the physiological activator, to point mutations of STIM proteins that disable Ca^{2+} sensing, chemically induced oligomerization of STIM, expression of cytosolic STIM fragments that activate Orai channels, 2-APB as a ligand for Orai3 channel activation, and now the identification of Orai1 gain-of-function mutants with altered gating and ion selectivity. We note that our results reveal a third way to open the Orai1 channel, each resulting in a distinct set of open channel characteristics. Activation of Orai1 by STIM1 or the smaller activating fragments yields a low-conductance, Ca^{2+}-selective pore with an inward rectifying I-V characteristic (26). Activation by 2-APB of Orai3 and, to a lesser extent, Orai1 yields a higher-conductance, nonselective cation pore with a biphasic I-V (22, 38). In contrast, the two G98 mutants exhibit spontaneous activity of a high-conductance, nonselective pore with a nearly linear I-V shape. These results provide clues to the molecular mechanism of CRAC channels and suggest directions for investigating the pathological roles of CRAC channels by overexpression of gain-of-function Orai1 mutants in different cell types. The fact that the G98 mutants reported here are single-point mutants further suggests the possibility of naturally occurring gain-of-function mutations in Orai1 with pathological consequences.

Materials and Methods

Cells. Human embryonic kidney (HEK)-293A cells obtained from Invitrogen were maintained in Dulbecco's modified Eagle medium (Lonza) supplemented with 10% fetal calf serum (Omega Scientific) and 2 mM L-glutamine (Sigma). HEK-293A cells were transfected using Lipofectamine 2000 (Invitrogen) or GenJet Plus (SignaGen Laboratories) reagents and used after 24 h for $[Ca^{2+}]_i$ imaging, immunocytochemistry, or Western blotting, and after 48–72 h for patch-clamp electrophysiology.

Molecular Cloning and Mutagenesis. The generation of *pcDNA3/humanSTIM1* and *pcDNA5/Myc-humanOrai1* and *eGFP-tagged humanOrai1* was described previously (6, 22, 39). All Orai1 mutants were created by exchanging the corresponding codons using the QuikChange Site-Directed Mutagenesis Kit (Stratagene). Information on primer design and conditions for cloning and PCR is available upon request.

Single-Cell $[Ca^{2+}]_i$ Imaging. Ratiometric $[Ca^{2+}]_i$ imaging was performed as described (22). Transfected cells were identified by the coexpressed GFP using filters to avoid contamination of fura-2 fluorescence by bleed-through of GFP fluorescence. Data were analyzed with Metafluor software (Universal Imaging) and OriginPro 7.5 software (OriginLab) and are expressed as means ± SE.

Diamide Assays. Two days after transfection, six-well dishes plated with HEK-293A cells were washed and then bathed in 2 mM Ca Ringer solution with or without diamide (10 mM final concentration) at room temperature for 30 min, followed by N-ethylmaleimide quenching (50 mM final concentration) at room temperature for 15 min. Cells were then washed with cold PBS and lysed in 300 μL of RIPA lysis buffer (Upstate) supplemented with 1× Complete EDTA-free protease inhibitor mixture (Roche Applied Science) and passed five times through a 26-gauge needle.

Whole-Cell Recording. Whole-cell recordings were done on transfected HEK-293A cells as described previously (11, 22), using procedures and solutions (Table S1) described in *SI Materials and Methods*.

ACKNOWLEDGMENTS. We thank Dr. Lu Forrest for assistance in cell culture and Dr. Michelle Digman and University of California, Irvine Developmental Biology Center Optical Biology Core Facility for technical support with confocal imaging. This work was supported by National Institutes of Health Grant NS-14609 (to M.D.C.) and the National Basic Research Program of China (973 Program; Grant 2010CB833702 to J.H.).

1. Parekh AB, Putney JW, Jr. (2005) Store-operated calcium channels. *Physiol Rev* 85: 757–810.
2. Cahalan MD, et al. (2007) Molecular basis of the CRAC channel. *Cell Calcium* 42: 133–144.
3. Feske S (2007) Calcium signalling in lymphocyte activation and disease. *Nat Rev Immunol* 7:690–702.
4. Feske S, et al. (2006) A mutation in Orai1 causes immune deficiency by abrogating CRAC channel function. *Nature* 441:179–185.
5. Liou J, et al. (2005) STIM is a Ca^{2+} sensor essential for Ca^{2+}-store-depletion-triggered Ca^{2+} influx. *Curr Biol* 15:1235–1241.
6. Roos J, et al. (2005) STIM1, an essential and conserved component of store-operated Ca^{2+} channel function. *J Cell Biol* 169:435–445.
7. Vig M, et al. (2006) CRACM1 is a plasma membrane protein essential for store-operated Ca^{2+} entry. *Science* 312:1220–1223.
8. Zhang SL, et al. (2006) Genome-wide RNAi screen of Ca^{2+} influx identifies genes that regulate Ca^{2+} release-activated Ca^{2+} channel activity. *Proc Natl Acad Sci USA* 103: 9357–9362.
9. Prakriya M, et al. (2006) Orai1 is an essential pore subunit of the CRAC channel. *Nature* 443:230–233.
10. Vig M, et al. (2006) CRACM1 multimers form the ion-selective pore of the CRAC channel. *Curr Biol* 16:2073–2079.
11. Yeromin AV, et al. (2006) Molecular identification of the CRAC channel by altered ion selectivity in a mutant of Orai. *Nature* 443:226–229.
12. Zhang SL, et al. (2005) STIM1 is a Ca^{2+} sensor that activates CRAC channels and migrates from the Ca^{2+} store to the plasma membrane. *Nature* 437:902–905.
13. Luik RM, Wang B, Prakriya M, Wu MM, Lewis RS (2008) Oligomerization of STIM1 couples ER calcium depletion to CRAC channel activation. *Nature* 454:538–542.
14. Prakriya M, Lewis RS (2006) Regulation of CRAC channel activity by recruitment of silent channels to a high open-probability gating mode. *J Gen Physiol* 128:373–386.
15. Yeromin AV, Roos J, Stauderman KA, Cahalan MD (2004) A store-operated calcium channel in *Drosophila* S2 cells. *J Gen Physiol* 123:167–182.
16. Zweifach A, Lewis RS (1993) Mitogen-regulated Ca^{2+} current of T lymphocytes is activated by depletion of intracellular Ca^{2+} stores. *Proc Natl Acad Sci USA* 90:6295–6299.
17. Gwack Y, et al. (2007) Biochemical and functional characterization of Orai proteins. *J Biol Chem* 282:16232–16243.
18. Mignen O, Thompson JL, Shuttleworth TJ (2008) Orai1 subunit stoichiometry of the mammalian CRAC channel pore. *J Physiol* 586:419–425.
19. Thompson JL, Mignen O, Shuttleworth TJ (2009) The Orai1 severe combined immune deficiency mutation and calcium release-activated Ca^{2+} channel function in the heterozygous condition. *J Biol Chem* 284:6620–6626.
20. Ji W, et al. (2008) Functional stoichiometry of the unitary calcium-release-activated calcium channel. *Proc Natl Acad Sci USA* 105:13668–13673.
21. Madl J, et al. (2010) Resting state Orai1 diffuses as homotetramer in the plasma membrane of live mammalian cells. *J Biol Chem* 285:41135–41142.
22. Zhang SL, et al. (2008) Store-dependent and -independent modes regulating Ca^{2+} release-activated Ca^{2+} channel activity of human Orai1 and Orai3. *J Biol Chem* 283: 17662–17671.
23. Byun M, et al. (2010) Whole-exome sequencing-based discovery of STIM1 deficiency in a child with fatal classic Kaposi sarcoma. *J Exp Med* 207:2307–2312.
24. Picard C, et al. (2009) STIM1 mutation associated with a syndrome of immunodeficiency and autoimmunity. *N Engl J Med* 360:1971–1980.
25. Derler I, et al. (2009) Increased hydrophobicity at the N terminus/membrane interface impairs gating of the severe combined immunodeficiency-related ORAI1 mutant. *J Biol Chem* 284:15903–15915.
26. Cahalan MD (2009) STIMulating store-operated Ca^{2+} entry. *Nat Cell Biol* 11:669–677.
27. Zhou Y, Ramachandran S, Oh-Hora M, Rao A, Hogan PG (2010) Pore architecture of the ORAI1 store-operated calcium channel. *Proc Natl Acad Sci USA* 107:4896–4901.
28. McNally BA, Yamashita M, Engh A, Prakriya M (2009) Structural determinants of ion permeation in CRAC channels. *Proc Natl Acad Sci USA* 106:22516–22521.
29. Penna A, et al. (2008) The CRAC channel consists of a tetramer formed by Stim-induced dimerization of Orai dimers. *Nature* 456:116–120.
30. Maruyama Y, et al. (2009) Tetrameric Orai1 is a teardrop-shaped molecule with a long, tapered cytoplasmic domain. *J Biol Chem* 284:13676–13685.
31. Payandeh J, Scheuer T, Zheng N, Catterall WA (2011) The crystal structure of a voltage-gated sodium channel. *Nature* 475:353–358.
32. Webster SM, Del Camino D, Dekker JP, Yellen G (2004) Intracellular gate opening in Shaker K^+ channels defined by high-affinity metal bridges. *Nature* 428:864–868.
33. Zhao Y, Yarov-Yarovoy V, Scheuer T, Catterall WA (2004) A gating hinge in Na^+ channels. *Neuron* 41:859–865.
34. Chen X, Aldrich RW (2011) Charge substitution for a deep-pore residue reveals structural dynamics during BK channel gating. *J Gen Physiol* 138:137–154.
35. Zhao Y, Scheuer T, Catterall WA (2004) Reversed voltage-dependent gating of a bacterial sodium channel with proline substitutions in the S6 transmembrane segment. *Proc Natl Acad Sci USA* 101:17873–17878.
36. Jiang Y, et al. (2002) Crystal structure and mechanism of a calcium-gated potassium channel. *Nature* 417:515–522.
37. Muik M, et al. (2011) STIM1 couples to ORAI1 via an intramolecular transition into an extended conformation. *EMBO J* 30:1678–1689.
38. Yamashita M, Somasundaram A, Prakriya M (2011) Competitive modulation of Ca^{2+} release-activated Ca^{2+} channel gating by STIM1 and 2-aminoethyldiphenyl borate. *J Biol Chem* 286:9429–9442.
39. Lioudyno MI, et al. (2008) Orai1 and STIM1 move to the immunological synapse and are up-regulated during T cell activation. *Proc Natl Acad Sci USA* 105:2011–2016.